Periodic inversion and phase transition of finite energy Airy beams in a medium with parabolic potential

Yiqi Zhang,[1,5] Milivoj R. Belić,[2,6] Lei Zhang,[3] Weiping Zhong,[4] Dayu Zhu,[1] Ruimin Wang,[1] and Yanpeng Zhang[1,7]

[1]*Key Laboratory for Physical Electronics and Devices of the Ministry of Education & Shaanxi Key Lab of Information Photonic Technique, Xi'an Jiaotong University, Xi'an 710049, China*
[2]*Science Program, Texas A&M University at Qatar, P.O. Box 23874 Doha, Qatar*
[3]*Department of Electrical and Computer Engineering, National University of Singapore, 4 Engineering Drive 3, Singapore 117583, Singapore*
[4]*Department of Electronic and Information Engineering, Shunde Polytechnic, Shunde 528300, China*
[5]*zhangyiqi@mail.xjtu.edu.cn*
[6]*milivoj.belic@qatar.tamu.edu*
[7]*ypzhang@mail.xjtu.edu.cn*

Abstract: We study periodic inversion and phase transition of normal, displaced, and chirped finite energy Airy beams propagating in a parabolic potential. This propagation leads to an unusual oscillation: for half of the oscillation period the Airy beam accelerates in one transverse direction, with the main Airy beam lobe leading the train of pulses, whereas in the other half of the period it accelerates in the opposite direction, with the main lobe still leading – but now the whole beam is inverted. The inversion happens at a critical point, at which the beam profile changes from an Airy profile to a Gaussian one. Thus, there are two distinct phases in the propagation of an Airy beam in the parabolic potential – the normal Airy and the single-peak Gaussian phase. The length of the single-peak phase is determined by the size of the decay parameter: the smaller the decay, the smaller the length. A linear chirp introduces a transverse displacement of the beam at the phase transition point, but does not change the location of the point. A quadratic chirp moves the phase transition point, but does not affect the beam profile. The two-dimensional case is discussed briefly, being equivalent to a product of two one-dimensional cases.

OCIS codes: (050.1940) Diffraction; (070.3185) Invariant optical fields; (070.0070) Fourier optics and signal processing; (050.1590) Chirping; (350.5500) Propagation.

References and links

1. G. A. Siviloglou and D. N. Christodoulides, "Accelerating finite energy Airy beams," Opt. Lett. **32**, 979–981 (2007).
2. G. Siviloglou, J. Broky, A. Dogariu, and D. Christodoulides, "Observation of accelerating Airy beams," Phys. Rev. Lett. **99**, 213901 (2007).
3. M. A. Bandres and J. C. Gutiérrez-Vega, "Airy-Gauss beams and their transformation by paraxial optical systems," Opt. Express **15**, 16719–16728 (2007).
4. T. J. Eichelkraut, G. A. Siviloglou, I. M. Besieris, and D. N. Christodoulides, "Oblique Airy wave packets in bidispersive optical media," Opt. Lett. **35**, 3655–3657 (2010).

#236354 - $15.00 USD Received 18 Mar 2015; revised 25 Mar 2015; accepted 26 Mar 2015; published 14 Apr 2015

5. N. K. Efremidis, "Airy trajectory engineering in dynamic linear index potentials," Opt. Lett. **36**, 3006–3008 (2011).
6. Y. Q. Zhang, M. Belić, Z. K. Wu, H. B. Zheng, K. Q. Lu, Y. Y. Li, and Y. P. Zhang, "Soliton pair generation in the interactions of Airy and nonlinear accelerating beams," Opt. Lett. **38**, 4585–4588 (2013).
7. R. Driben, Y. Hu, Z. Chen, B. A. Malomed, and R. Morandotti, "Inversion and tight focusing of Airy pulses under the action of third-order dispersion," Opt. Lett. **38**, 2499–2501 (2013).
8. W.-P. Zhong, M. Belić, Y. Q. Zhang, and T. Huang, "Accelerating Airy-Gauss-Kummer localized wave packets," Ann. Phys. **340**, 171–178 (2014).
9. Y. Q. Zhang, M. R. Belić, H. B. Zheng, H. X. Chen, C. B. Li, Y. Y. Li, and Y. P. Zhang, "Interactions of Airy beams, nonlinear accelerating beams, and induced solitons in Kerr and saturable nonlinear media," Opt. Express **22**, 7160–7171 (2014).
10. I. Besieris and A. Shaarawi, "Accelerating Airy wave packets in the presence of quadratic and cubic dispersion," Phys. Rev. E **78**, 046605 (2008).
11. R. Driben and T. Meier, "Regeneration of Airy pulses in fiber-optic links with dispersion management of the two leading dispersion terms of opposite signs," Phys. Rev. A **89**, 043817 (2014).
12. S. Wang, D. Fan, X. Bai, and X. Zeng, "Propagation dynamics of Airy pulses in optical fibers with periodic dispersion modulation," Phys. Rev. A **89**, 023802 (2014).
13. J. Rogel-Salazar, H. A. Jiménez-Romero, and S. Chávez-Cerda, "Full characterization of Airy beams under physical principles," Phys. Rev. A **89**, 023807 (2014).
14. G. Zhou, R. Chen, and G. Ru, "Propagation of an Airy beam in a strongly nonlocal nonlinear media," Laser Phys. Lett. **11**, 105001 (2014).
15. W. Liu, D. N. Neshev, I. V. Shadrivov, A. E. Miroshnichenko, and Y. S. Kivshar, "Plasmonic Airy beam manipulation in linear optical potentials," Opt. Lett. **36**, 1164–1166 (2011).
16. Z. Ye, S. Liu, C. Lou, P. Zhang, Y. Hu, D. Song, J. Zhao, and Z. Chen, "Acceleration control of Airy beams with optically induced refractive-index gradient," Opt. Lett. **36**, 3230–3232 (2011).
17. F. Xiao, B. Li, M. Wang, W. Zhu, P. Zhang, S. Liu, M. Premaratne, and J. Zhao, "Optical Bloch oscillations of an Airy beam in a photonic lattice with a linear transverse index gradient," Opt. Express **22**, 22763–22770 (2014).
18. A. W. Snyder and D. J. Mitchell, "Accessible solitons," Science **276**, 1538–1541 (1997).
19. S. Ponomarenko and G. Agrawal, "Do solitonlike self-similar waves exist in nonlinear optical media?" Phys. Rev. Lett. **97**, 013901 (2006).
20. W. Zhong and L. Yi, "Two-dimensional Laguerre-Gaussian soliton family in strongly nonlocal nonlinear media," Phys. Rev. A **75**, 061801 (2007).
21. B. Yang, W.-P. Zhong, and M. R. Belić, "Self-similar Hermite-Gaussian spatial solitons in two-dimensional nonlocal nonlinear media," Commun. Theor. Phys. **53**, 937–942 (2010).
22. G. Agarwal and R. Simon, "A simple realization of fractional Fourier transform and relation to harmonic oscillator Green's function," Opt. Commun. **110**, 23–26 (1994).
23. C. Bernardini, F. Gori, and M. Santarsiero, "Converting states of a particle under uniform or elastic forces into free particle states," Eur. J. Phys **16**, 58–62 (1995).
24. H. M. Ozaktas, Z. Zalevsky, and M. A. Kutay, *The Fractional Fourier Transform with Applications in Optics and Signal Processing* (Wiley, New York, 2001).
25. O. Vallée and M. Soares, *Airy functions and applications to physics* (Imperial College Press, Singapore, 2010), 2nd ed.
26. Y. Q. Zhang, M. R. Belić, H. B. Zheng, Z. K. Wu, Y. Y. Li, K. Q. Lu, and Y. P. Zhang, "Fresnel diffraction patterns as accelerating beams," Europhys. Lett. **104**, 34007 (2013).
27. L. Zhang, K. Liu, H. Zhong, J. Zhang, Y. Li, and D. Fan, "Effect of initial frequency chirp on Airy pulse propagation in an optical fiber," Opt. Express **23**, 2566–2576 (2015).
28. G. A. Siviloglou, J. Broky, A. Dogariu, and D. N. Christodoulides, "Ballistic dynamics of Airy beams," Opt. Lett. **33**, 207–209 (2008).
29. Y. Hu, P. Zhang, C. Lou, S. Huang, J. Xu, and Z. Chen, "Optimal control of the ballistic motion of Airy beams," Opt. Lett. **35**, 2260–2262 (2010).
30. R. Driben, V. V. Konotop, and T. Meier, "Coupled Airy breathers," Opt. Lett. **39**, 5523–5526 (2014).

1. Introduction

Airy beams exhibiting accelerating, nondiffracting and self–healing properties have become a subject of immense interest in the last decade [1–9]. Among research topics, the propagation of Airy beams in optical fibers has attracted much attention recently [7, 10–12]. There, taking the third-order dispersion into account results in pulses resisting dispersive distortion, performing transverse inversion, and producing oscillating behavior. Such an inversion of an Airy beam occurring during propagation can also be obtained from the double focusing effect [13] or in

#236354 - $15.00 USD Received 18 Mar 2015; revised 25 Mar 2015; accepted 26 Mar 2015; published 14 Apr 2015

a strongly nonlocal nonlinear medium [14]. Similar to traditional beams, the dynamics of an Airy beam may easily be manipulated in the presence of an external potential. For example, due to a linear potential, the accelerating trajectory of an Airy beam can be stretched transversely [5,15,16]. Bloch oscillation and Zener tunneling of an Airy beam can be obtained in a photonic lattice [17], to name a few solid-state-like phenomena.

Here, we are specifically concerned with what happens in an external parabolic potential – a workhorse of the introductory quantum mechanics. Although the quantum-mechanical harmonic oscillator is a well-researched topic, in paraxial optics sometimes it leads to unexpected novel propagation phenomena. This potential – among myriad of other uses – is frequently utilized as a harmonic trap in Bose-Einstein condensates, especially if the nonlinearity is weak and can be neglected. Another nonlinear problem which easily turns linear is the beam propagation in highly nonlocal media, such as nematic liquid crystals. The accessible soliton model of Snyder and Mitchel [18] in the highly nonlocal limit reduces to the linear harmonic oscillator. A widely used application of the parabolic potential in optics is in the propagation of pulses in graded-index (GRIN) fibers. If one launches a Gaussian beam into such a potential, it oscillates back and forth without changing its profile, in a perfect harmonic style. However, if one launches an Airy beam in a parabolic potential, the propagation is very different.

Quite surprisingly, such a problem has not been considered in the research literature. Linear dynamics of an Airy-Gauss beam due to a parabolic potential was addressed in [3], using the ABCD matrix method. However, in view of the importance of Airy and related diffraction-free beams, the topic deserves deeper exploration. Owing to the parabolic potential, a finite energy Airy beam will undergo a profound change, including periodic inversion during propagation and curious shape change at the critical – turning – points. This motion is *not* the harmonic oscillation. Such a behavior raises a number of questions. The most obvious is, why and how does the inversion happen? How to understand and describe the process? What happens at the critical point? Does the beam remain diffraction-free? Is the inversion affected by a transverse displacement of the beam? These questions will be addressed in this paper.

We investigate here the linear dynamics of normal and transversely displaced Airy beams due to a parabolic potential, theoretically and numerically. We answer the questions posed above. However, one should keep in mind that these questions pertain to the motion of the lobes or of the caustics of an Airy beam – which is what people usually have in mind when talking about the accelerating beams. The center of mass of a finite energy Airy beam follows different dynamics – in this case a perfect harmonic oscillation. This is the same motion as that of a Gaussian beam in parabolic potential – except that the Gaussian beam does not change its shape while oscillating, whereas the Airy beam changes drastically.

The organization of the paper is as follows. In Sec. 2, we introduce the theoretical model; in Sec. 3, we find an analytical solution when the initial beam is a transversely displaced finite energy Airy beam; and in Sec. 4 we provide the solution when the initial beam is chirped. The two–dimensional case is briefly discussed in Sec. 5. We conclude the paper in Sec. 6.

2. Theoretical model

In the paraxial approximation and in the absence of nonlinearity, the beam in propagation obeys the normalized dimensionless linear parabolic (Schrödinger-like) equation

$$i\frac{\partial \psi}{\partial z} + \frac{1}{2}\frac{\partial^2 \psi}{\partial x^2} - V(x)\psi = 0, \tag{1}$$

where ψ is the beam envelope and $V(x)$ an external potential, usually coming from an appropriate change in the medium's refractive index. The variables x and z are the normalized transverse coordinate and the propagation distance, scaled by some characteristic transverse width x_0 and

#236354 - $15.00 USD Received 18 Mar 2015; revised 25 Mar 2015; accepted 26 Mar 2015; published 14 Apr 2015

the corresponding Rayleigh range kx_0^2. Here, $k = 2\pi n/\lambda_0$ is the wavenumber, n the index of refraction, and λ_0 the wavelength in free space. For our purpose, the values of parameters can be taken as $x_0 = 100\,\mu$m, and $\lambda_0 = 600\,$nm [6, 9]. We consider the parabolic potential

$$V(x) = \frac{1}{2}\alpha^2 x^2$$

with the parameter α measuring the depth of the potential.

With this choice of the potential, Eq. (1) describes the linear harmonic oscillator and possesses many well-known solutions. We select the ones that are relevant for the study at hand, some of which are derived by the self-similar method [19–21]. Generally, the solution of Eq. (1) can be written as [22, 23]

$$\psi(x, z) = \int_{-\infty}^{+\infty} \psi(\xi, 0)\sqrt{\mathscr{H}(x, \xi, z)}d\xi, \tag{2}$$

where

$$\mathscr{H}(x, \xi, z) = -\frac{i}{2\pi}\alpha \csc(\alpha z) \exp\left\{i\alpha \cot(\alpha z)\left[x^2 + \xi^2 - 2x\xi \sec(\alpha z)\right]\right\} \tag{3}$$

is associated with the corresponding kernel. Combining Eqs. (2) and (3), after some algebra one ends up with

$$\psi(x, z) = f(x, z)\int_{-\infty}^{+\infty}\left[\psi(\xi, 0)\exp\left(ib\xi^2\right)\right]\exp(-iK\xi)d\xi, \tag{4}$$

where $b = \frac{\alpha}{2}\cot(\alpha z)$, $K = \alpha x \csc(\alpha z)$, and

$$f(x, z) = \sqrt{-\frac{i}{2\pi}\frac{K}{x}}\exp\left(ibx^2\right).$$

One can see that the integral in Eq. (4) is a Fourier transform of $\psi(x, 0)\exp(ibx^2)$, with K being the spatial frequency. Therefore, after choosing a certain input $\psi(x, 0)$, one can get an analytical evolution solution by finding the Fourier transform of $\psi(x, 0)\exp(ibx^2)$. In other words, the propagation of a beam in a parabolic potential is equivalent to the self-Fourier transform; that is, to a periodic change from the beam to the Fourier transform of the beam with quadratic chirp and back. It is worth mentioning that Eq. (4) is a fractional Fourier transform of the initial beam [24], the "degree" of which is proportional to the propagation distance. Overall, the use of Fourier transform simplifies the analysis greatly.

3. Solutions and numerical simulations

3.1. Finite energy Airy beams without transverse displacement

We consider first the case in which a finite energy Airy beam $\psi(x, 0) = \mathrm{Ai}(x)\exp(ax)$ is the input, where a is the decay parameter – a positive real number which makes the total energy finite. It also makes the beam more easily fit into the potential well. The solution of Eq. (4) can be found using two steps:

(i) Find the Fourier transforms of $\psi(x, 0) = \mathrm{Ai}(x)\exp(ax)$ and $\exp(ibx^2)$, which can be written as [1, 2]:

$$\hat{\psi}(k) = \exp\left(-ak^2\right)\exp\left[\frac{a^3}{3} + \frac{i}{3}\left(k^3 - 3a^2k\right)\right], \tag{5a}$$

#236354 - $15.00 USD Received 18 Mar 2015; revised 25 Mar 2015; accepted 26 Mar 2015; published 14 Apr 2015

and

$$\sqrt{i\frac{\pi}{b}}\exp\left(-\frac{i}{4b}k^2\right), \tag{5b}$$

respectively.

(ii) Perform the convolution of the two Fourier transforms in Eqs. (5a) and (5b), and using the definition [25]

$$\mathrm{Ai}(x)=\frac{1}{2\pi i}\int_{-i\infty}^{+i\infty}\exp\left(xt-\frac{t^3}{3}\right)dt,$$

find the inverse Fourier transform:

$$\begin{aligned}\psi(x,z)=&-f(x,z)\sqrt{i\frac{\pi}{b}}\exp\left(\frac{a^3}{3}\right)\mathrm{Ai}\left(\frac{K}{2b}-\frac{1}{16b^2}+i\frac{a}{2b}\right)\\&\times\exp\left[\left(a+\frac{i}{4b}\right)\left(\frac{K}{2b}-\frac{1}{16b^2}+i\frac{a}{2b}\right)\right]\\&\times\exp\left[-i\frac{K^2}{4b}-\frac{1}{3}\left(a+\frac{i}{4b}\right)^3\right].\end{aligned} \tag{6}$$

This is the general procedure for solving Eq. (4). It is clear that the solution in Eq. (6) is a periodic function that should execute harmonic oscillation, as demanded by the parabolic potential. The question is, does this really happen?

From Eq. (6), one can find the accelerating trajectory of the initial beam during propagation, in the form:

$$x=\frac{1}{4\alpha^2}\frac{\sin^2(\alpha z)}{\cos(\alpha z)}, \tag{7}$$

with $z\neq(2m+1)\mathscr{D}/4$. Note that the trajectory in Eq. (7) is ideal, because it indicates that the Airy beam can accelerate all the way to infinity $x\to\pm\infty$ when $z\to(2m+1)\mathscr{D}/4$. However, upon exponential apodization of the Airy beam, such an acceleration will stop when z is close to the phase transition point $(2m+1)\mathscr{D}/4$. At that point the character of the beam propagation will drastically change – the beam will turn around, accelerate in the opposite direction, and change the shape. While the change in the sign of velocity is expected at the turning points of a parabolic potential, no change in the acceleration and shape is expected, nor the appearance of a different phase in the motion. Note also that the accelerating trajectory given by Eq. (7) is a periodic function, with the period

$$\mathscr{D}=\frac{2\pi}{\alpha}, \tag{8}$$

and not a parabolic curve.

Now, several issues concerning Eq. (6) must be addressed:

(i) When the propagation distance is an integer multiple of the period, i.e., $z=m\mathscr{D}$ with m being a nonnegative integer, we have $\psi(x,z)=\psi(x,0)$ – an initial beam recurrence.

(ii) When the propagation distance is an odd integer multiple of the period halves, i.e., $z=(2m+1)\mathscr{D}/2$, we have $\psi(x,z)=\psi(-x,0)$ – an inversion of the initial beam.

(iii) When the propagaion distance is an odd integer multiple of the period quarters, i.e. $z=(2m+1)\mathscr{D}/4$, we have trouble – Eq. (6) is invalid because $b=0$. In this case, one has to

#236354 - $15.00 USD Received 18 Mar 2015; revised 25 Mar 2015; accepted 26 Mar 2015; published 14 Apr 2015

directly solve Eq. (4) for the Fourier transform of the initial beam. The result is:

$$\psi\left(x, z=\frac{2m+1}{4}\mathscr{D}\right)=\sqrt{-i\frac{s\alpha}{2\pi}}\exp\left(-a\alpha^2x^2\right)\exp\left[\frac{a^3}{3}+i\frac{s}{3}\left(\alpha^3x^3-3a^2\alpha x\right)\right], \quad (9)$$

where $s=1$ if m is even and $s=-1$ if m is odd. This field is unrelated to the initial Airy beam – that is, a new "phase" of the propagating beam.

Interestingly, Eq. (9) displays a Gaussian intensity profile (energy distribution is parity-symmetric), which is completely different from the intensity profiles elsewhere during propagation (energy distribution is parity-asymmetric). It is similar to the propagating Gaussian pulse as it bounces off the potential wall – but the Gaussian beam remains Gaussian in propagation, whereas this pulse inverts and becomes an inverse Airy beam. On the other hand, it is different from a free Gaussian wave packet hitting an infinite potential wall – there, during the bounce the packet becomes rapidly oscillating multi-peaked structure, owing to the interference between the incoming and the reflected beam. Since the inversion introduces a discontinuity in the velocity and a singularity in the acceleration, for a lack of better word we refer to the phenomenon as the *phase transition* of the finite energy Airy beam, due to the parabolic potential. Correspondingly, $z=(2m+1)\mathscr{D}/4$ are the phase transition points.

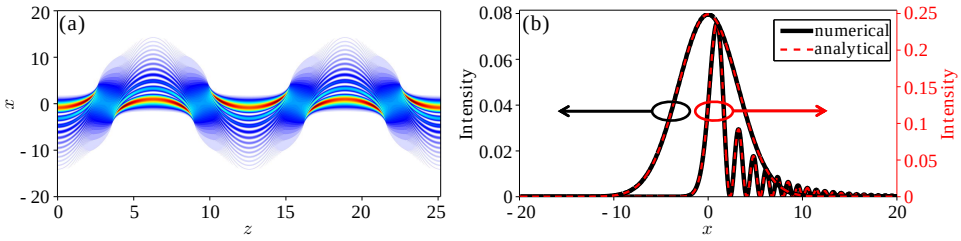

Fig. 1. (a) Propagation of a finite energy Airy beam $\psi(x,0)=\mathrm{Ai}(x)\exp(ax)$ with $a=0.1$ in a parabolic potential with $\alpha=0.5$ (Media 1). (b) Intensity profiles at $z=\mathscr{D}/4$ and $z=\mathscr{D}/2$, respectively. Solid and dashed curves represent the numerical simulation and the analytical solutions, respectively. Gaussian and Airy profiles refer to the left y-axis and the right y-axis, respectively, as indicated by the circle-arrows.

Following the aforementioned procedure, the solution involving propagation of a finite energy Airy beam is obtained, which is a combination of Eqs. (6) and (9). In Fig. 1(a) and Media 1, we show the propagation of the input Airy beam obtained numerically, using a beam propagation method; we set the propagation distance to only $2\mathscr{D}$, which is enough to display periodicity. One can see that the beam exhibits oscillation and periodic inversion during propagation, which is in accordance with the mentioned analytical prediction. But, the oscillation is not harmonic. One can also see that the propagation proceeds in a diffraction-free manner, the beam staying localized at all times. Here, we would like to point out that as α becomes smaller, the potential well becomes shallower, and the period becomes longer. Then, one essentially deals with the free space propagation and the beam must sustain a considerable diffraction for the positive parameter a. To make a comparison between the analytical and numerical results, we display in Fig. 1(b) the intensity profiles at $z=\mathscr{D}/4$ and $z=\mathscr{D}/2$, from which one can observe that the analytical (dashed curves) and numerical (solid curves) results agree with each other very well.

3.2. *Finite energy Airy beams with transverse displacement*

In this subsection we consider transversely displaced finite energy Airy beams. We introduce a transverse displacement x_0 to the beam, and write the initial beam as $\psi(x,0)=$

#236354 - $15.00 USD Received 18 Mar 2015; revised 25 Mar 2015; accepted 26 Mar 2015; published 14 Apr 2015

$\mathrm{Ai}(x-x_0)\exp[a(x-x_0)]$. The corresponding Fourier transform is written as

$$\hat{\psi}(k) = \exp(-ix_0k)\exp\left(-ak^2\right)\exp\left[\frac{a^3}{3}+\frac{i}{3}\left(k^3-3a^2k\right)\right], \tag{10}$$

according to the translation property of the Fourier transform. The general solution corresponding to this initial beam can be written as

$$\begin{aligned}\psi(x,z) = &-f(x,z)\sqrt{i\frac{\pi}{b}}\exp\left(\frac{a^3}{3}\right)\mathrm{Ai}\left(\frac{K}{2b}-\frac{1}{16b^2}+i\frac{a}{2b}-x_0\right)\\ &\times\exp\left[\left(a+\frac{i}{4b}\right)\left(\frac{K}{2b}-\frac{1}{16b^2}+i\frac{a}{2b}-x_0\right)\right]\\ &\times\exp\left[-i\frac{K^2}{4b}-\frac{1}{3}\left(a+\frac{i}{4b}\right)^3\right],\end{aligned} \tag{11}$$

from which one can see that the period does not change and that the beam still displays a phase transition at $z=(2m+1)\mathscr{D}/4$. Again, we can find the solution directly from Eq. (4), to obtain:

$$\psi\left(x, z=\frac{2m+1}{4}\mathscr{D}\right) = \sqrt{-i\frac{s\alpha}{2\pi}}\exp(-ix_0\alpha x)\exp\left(-a\alpha^2x^2\right)\exp\left[\frac{a^3}{3}+i\frac{s}{3}\left(\alpha^3x^3-3a^2\alpha x\right)\right]. \tag{12}$$

Comparing Eq. (12) with Eq. (9), one can see that the transverse displacement introduces a linear chirp to the solution at the phase transition point. The beam executes the same motion as before, but it is transversely stretched.

Overall, with the transversely displaced finite energy Airy beam as an input, the solution is a combination of Eqs. (11) and (12). The accelerating trajectory corresponding to this case is

$$x = \frac{1}{4\alpha^2}\frac{\sin^2(\alpha z)}{\cos(\alpha z)}+x_0\cos(\alpha z), \tag{13}$$

in which the second term on the right-hand side comes from the transverse displacement. One can predict that with increasing transverse displacement $|x_0|$, the beam will accelerate along an ever more elongated cosine curve. Note that the solution in Sec. 3.1 is a special case of the one found here, with $x_0=0$.

In Fig. 2, we display the propagation scenarios for a finite energy Airy beam propagating with different transverse displacements. Figures 2(a1)-2(a3) are for the cases with $x_0<0$, while Figs. 2(b1)-2(b3) are for the cases with $x_0>0$. In comparison with Fig. 1(a), the accelerating trajectories are modulated, due to the transverse displacement. Specifically, the beam with $x_0<0$ accelerates opposite to the case with $x_0\geq 0$; in Fig. 2(b3), the main lobe almost moves along a straight line. In addition, the accelerating trajectory indeed approaches the cosine-like curve for large $|x_0|$, as in Fig. 2(a1), in which $x_0=-15$. To elucidate the evolution clearly, Media 2 and Media 3 are prepared, corresponding to Figs. 2(a3) and 2(b3).

From Figs. 1(a) and 2, one can observe that some distance before and after the phase transition point the beam looses its multi-peak profile and propagates as an asymmetric single-hump beam. Only at the critical point it possesses a symmetric Gaussian profile. This phenomenon is a consequence of the beam approaching and bouncing off the potential wall. Owing to its finite energy, the beam spends some time at the turning point, and while bouncing off the potential wall it propagates as a single-peak pulse. To explore the phase transition region more clearly, we show the trajectories, velocities, and accelerations of the beam during propagation in Fig.

#236354 - $15.00 USD Received 18 Mar 2015; revised 25 Mar 2015; accepted 26 Mar 2015; published 14 Apr 2015

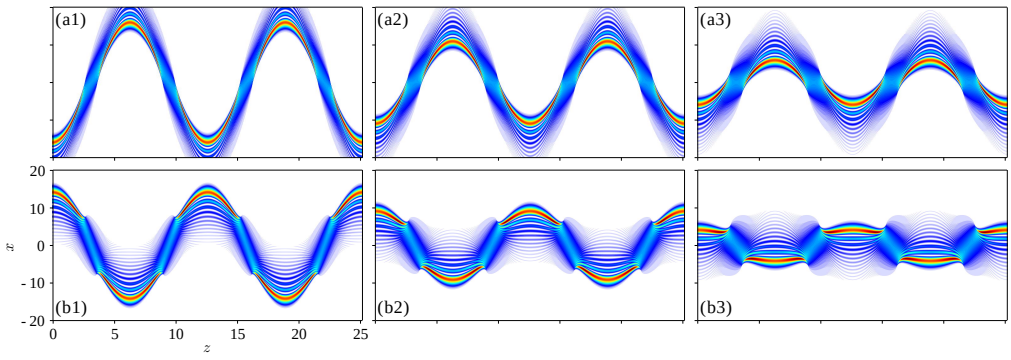

Fig. 2. Propagation of finite energy Airy beams with different transverse displacements. (a1)-(a3) $x_0 = -15$, -10, and -5, respectively (Media 2). (b1)-(b3) $x_0 = 15$, 10, and 5, respectively (Media 3). Other parameters are $a = 0.1$ and $\alpha = 0.5$.

3, for different cases. The curves in the left column of the figure display the dynamics of the maximum of the beam intensity captured numerically, while the curves in the right column are the analytical results obtained according to Eqs. (7) and (13). The figure nicely displays why the motion is not harmonic. If it were harmonic, the curves for trajectories would be the same as those for accelerations, but of the opposite sign and scaled by a factor – and they are not. In fact, for the beam without displacement, the position and acceleration are *of the same sign*. Also, note the fundamental difference between the numerical and analytical curves – the numerical ones predict two-phase dynamics, whereas the analytical do not. Based on the numerical curves, one can see that the beam indeed displays two phase regions during propagation – the Airy phase and the single-peak phase. However, based on the analytical curves, one can argue in the opposite as well.

According to Eqs. (11) and (12), the single-peak structure only occurs at the phase transition points; before and after these points, the beam still exhibits multi-peak structure, but the peaks are too small to recognize. This is quite similar to the case of Fresnel diffraction patterns considered as accelerating beams, in which the pattern decelerates first, then accumulates at the edge (at a certain point), loses its multi-peak structure, and finally accelerates in the opposite direction [26]. Strictly speaking, there is no single-peak phase region except at the phase transition point; however, the system has to reconnect the accelerating motion before the point with the decelerating motion after the point. In the tiny region around phase transition points, the motion of the beam is qualitatively different from that of the beam in the Airy phase. This is why numerical and analytical results agree with each other very well in the Airy phase region, while in the single-peak region, they do not. On the other hand, the analytical trajectory, velocity, and acceleration tend to infinity when the beam approaches the phase transition point, according to Figs. 3(b1)-3(b3). This goes against physical reality. Oscillation requires bounded trajectory, velocity, and acceleration. Thus, the results with an apodization are more realistic.

It is interesting to compare this motion with the motion of *the center of "mass"*, defined as

$$\bar{x} = \frac{\int_{-\infty}^{+\infty} x|\psi(x)|^2 dx}{\int_{-\infty}^{+\infty} |\psi(x)|^2 dx}.$$

As mentioned, we find that the oscillation of the center of the mass is harmonic (not shown). More accurately, the whole wavepacket undergoes harmonic oscillation in a parabolic potential, but the maximum of the beam intensity does not.

#236354 - $15.00 USD Received 18 Mar 2015; revised 25 Mar 2015; accepted 26 Mar 2015; published 14 Apr 2015

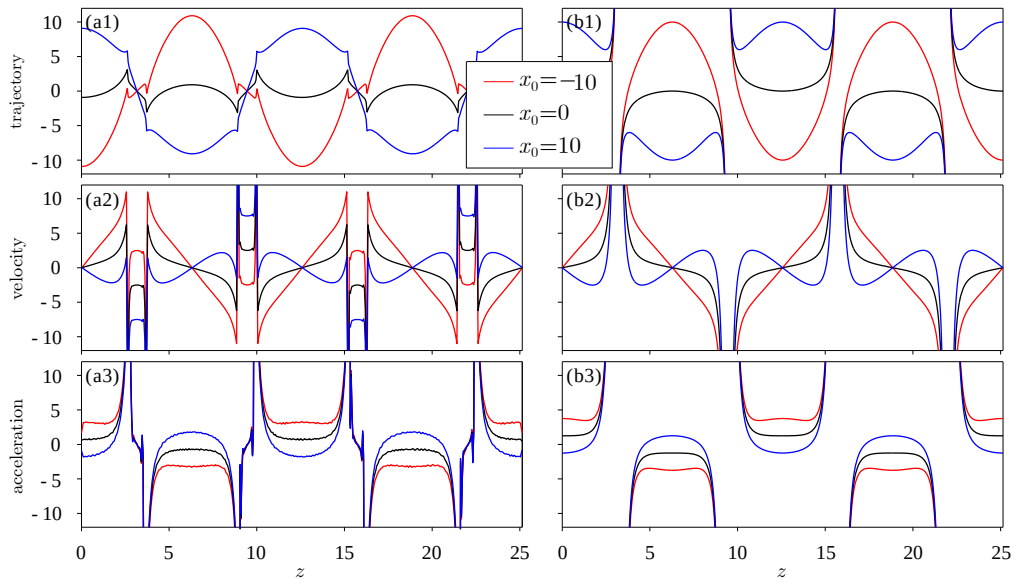

Fig. 3. (a) Numerical trajectory (a1), velocity (a2) and acceleration (a3) of the Airy beam during propagation. Red, black and blue curves correspond to the transversely displaced beams, with displacements $x_0 = -10$, 0, and 10, respectively. (b) Analytical trajectory (b1), velocity (b2) and acceleration (b3) corresponding to (a). Other parameters are $a = 0.1$ and $\alpha = 0.5$.

According to Eq. (13), the trajectory is independent of the decay parameter a. Nevertheless, the single-peak region does depend on a. To perform an exact analysis of the relation between the width of the region and a from Eq. (11) is not an easy task. Therefore, we only present this relation numerically; the result is shown in Fig. 4(a). As one could predict, the single-peak phase region increases with a increasing. The smaller the decay parameter, the harder for the beam to make a sudden inversion. In a similar vein, the transverse displacement x_0 does not affect the width of the single-peak phase region when a is fixed. In Figs. 4(b) and 4(c), corresponding to the two dots shown in Fig. 4(a), we display another two cases of the finite energy Airy beam propagation without transverse displacement (viz. $x_0 = 0$) over a half of the period, with $a = 0.01$ and 0.05, respectively. Clearly, one can see that the single-peak phase region in Fig. 4(b) is narrower than that in Fig. 4(c).

4. Chirped finite energy Airy beams

According to Eq. (4), the beam propagation is equivalent to the Fourier transform of an initial beam with a quadratic chirp; thus, we wonder what is the dynamics of the chirped finite energy Airy beams. In this subsection, we address this topic and consider two cases: the linearly chirped beam and the quadratically chirped beam. The propagation of a chirped Airy beam in an optical fiber was recently reported in [27], in which a relation between the second-order dispersion parameter and the chirp was displayed.

4.1. Linearly chirped beam

The finite energy Airy beam with a linear chirp is written as

$$\psi(x, 0) = \mathrm{Ai}(x - x_0)\exp[a(x - x_0)]\exp(i\beta x),$$

#236354 - $15.00 USD Received 18 Mar 2015; revised 25 Mar 2015; accepted 26 Mar 2015; published 14 Apr 2015

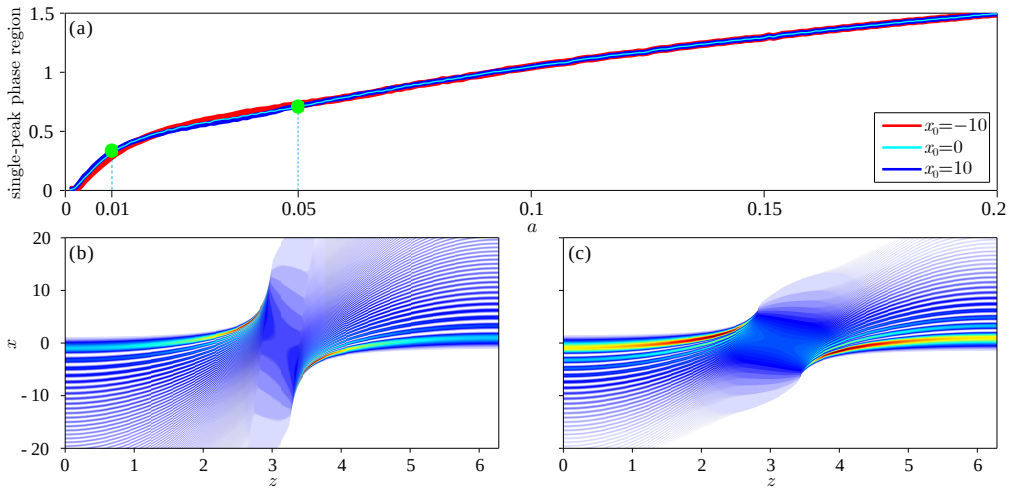

Fig. 4. (a) The width of the single-peak phase region versus the decay parameter a, corresponding to Fig. 3. (b) and (c) Same as Fig. 1(a), but over a half of the period and corresponding to the green dots in (a). In the left panel, $a = 0.01$; in the right, $a = 0.05$.

with β being the constant wavenumber. Clearly, the linear chirp will lead to a displacement β in the spatial frequency domain. Thus, according to Eqs. (11) and (12), one can write the solution as

$$\begin{aligned}\psi(x,z) = &- f(x,z)\sqrt{i\frac{\pi}{b}}\exp\left(\frac{a^3}{3}\right)\mathrm{Ai}\left(\frac{K'}{2b}-\frac{1}{16b^2}+i\frac{a}{2b}-x_0\right)\\ &\times\exp\left[\left(a+\frac{i}{4b}\right)\left(\frac{K'}{2b}-\frac{1}{16b^2}+i\frac{a}{2b}-x_0\right)\right]\\ &\times\exp\left[-i\frac{K'^2}{4b}-\frac{1}{3}\left(a+\frac{i}{4b}\right)^3\right],\end{aligned}\tag{14a}$$

with $K' = K - \beta$. It is clear that the period $\mathscr{D}$ does not change and the phase transition point is still an odd integer multiple of the quarters of the period. At the phase transition point, we have

$$\begin{aligned}\psi\left(x, z=\frac{2m+1}{4}\mathscr{D}\right) = &\sqrt{-i\frac{s\alpha}{2\pi}}\exp[-ix_0(\alpha x-\beta)]\exp\left[-a(\alpha x-\beta)^2\right]\\ &\times\exp\left\{\frac{a^3}{3}+i\frac{s}{3}\left[(\alpha x-\beta)^3-3a^2(\alpha x-\beta)\right]\right\}.\end{aligned}\tag{14b}$$

In Fig. 5 the intensities of linearly chirped finite energy Airy beams with different transverse displacements are displayed as functions of the propagation distance (Media 4 corresponds to Fig. 5(b)). In the figure, $\beta = 5$ is fixed, while the displacements vary from -10 to 10. In comparison with the results shown in Fig. 2, one can see that both the period and the phase transition point do not change, but the central point of the beam profile changes, which agrees well with the analytical results.

It is worth mentioning that the beam with a linear chirp is equivalent to an obliquely incident beam. For an obliquely incident Airy beam in free space, it is well known that it exhibits ballistic properties resembling a projectile motion [28,29]. However, such ballistic properties are absent in the presence of a parabolic potential, as shown in Fig. 5. In comparison with Figs. 1(a), 2(a2)

#236354 - $15.00 USD Received 18 Mar 2015; revised 25 Mar 2015; accepted 26 Mar 2015; published 14 Apr 2015

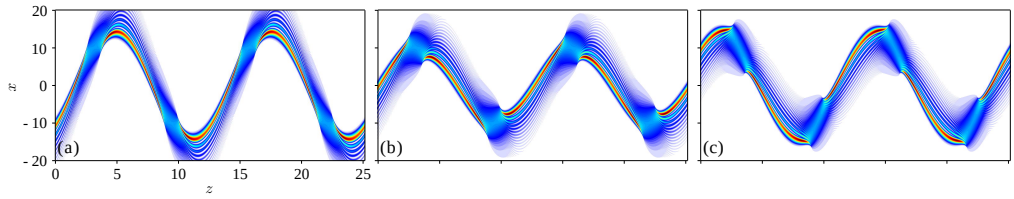

Fig. 5. Propagation of finite energy Airy beams with a linear chirp and different transverse displacements. (a)-(c) $x_0 = -10$, 0, and 10, respectively (Media 4). Other parameters are $a = 0.1$, $\alpha = 0.5$, and $\beta = 5$.

and 2(b2), we find that the trajectories in Fig. 5 are modulated greatly. Mathematically, the trajectory is given by

$$x = \frac{1}{4\alpha^2}\frac{\sin^2(\alpha z)}{\cos(\alpha z)} + x_0\cos(\alpha z) + \frac{\beta}{\alpha}\sin(\alpha z), \tag{15}$$

where the third term on the right-hand side comes from the linear chirp.

4.2. *Quadratically chirped beam*

If the initial finite energy Airy beam carries a quadratic chirp, it can be written in the form:

$$\psi(x,0) = \mathrm{Ai}(x-x_0)\exp\left[a(x-x_0)\right]\exp\left(i\beta x^2\right).$$

Plugging this initial beam into Eq. (4), we end up with

$$\psi(x,z) = f(x,z)\int_{-\infty}^{+\infty}\left[\psi(\xi,0)\exp\left(ib'\xi^2\right)\right]\exp(-iK\xi)d\xi, \tag{16}$$

with $b' = b+\beta$. This solution is still the Fourier transform of the initial beam with a quadratic chirp. Thus, based on Eq. (11), the analytical solution can be written as

$$\begin{aligned}\psi(x,z) = &-f(x,z)\sqrt{i\frac{\pi}{b'}}\exp\left(\frac{a^3}{3}\right)\mathrm{Ai}\left(\frac{K}{2b'}-\frac{1}{16b'^2}+i\frac{a}{2b'}-x_0\right)\\ &\times\exp\left[\left(a+\frac{i}{4b'}\right)\left(\frac{K}{2b'}-\frac{1}{16b'^2}+i\frac{a}{2b'}-x_0\right)\right]\\ &\times\exp\left[-i\frac{K^2}{4b'}-\frac{1}{3}\left(a+\frac{i}{4b'}\right)^3\right].\end{aligned} \tag{17}$$

Since β is a constant, the period of Eq. (17) is still $\mathscr{D}$. However, the phase transition point is not the same. If we let $b' = 0$, the phase transition point is obtained as

$$z = \frac{1}{\alpha}\arctan\left(-\frac{\alpha}{2\beta}\right) + \frac{m}{2}\mathscr{D}. \tag{18}$$

If we let $\beta \to 0$ in Eq. (18), the phase transition point tends to $(2m+1)\mathscr{D}/4$. In light of the fact that the beam at the phase transition point is still the Fourier transform of the initial beam excluding the quadratic chirp, the beam at this point can be still depicted by Eq. (12). As to the trajectory, it is now

$$x = \frac{\sin^2(\alpha z)}{4\alpha[\alpha\cos(\alpha z)+2\beta\sin(\alpha z)]} + [\alpha\cos(\alpha z)+2\beta\sin(\alpha z)]x_0. \tag{19}$$

#236354 - $15.00 USD Received 18 Mar 2015; revised 25 Mar 2015; accepted 26 Mar 2015; published 14 Apr 2015

In comparison with the trajectories shown in Eqs. (13) and (15), the influence from the quadratic chirp is not negligible; it is connected with the two terms on the right-hand side in Eq. (13). On the other hand, the phase transition point of Eq. (19) is not $z = (2m+1)\mathscr{D}/4$ any longer, as it was in Eqs. (7), (13) and (15). Actually, the point can be obtained after an involved algebra, and is the one displayed in Eq. (18).

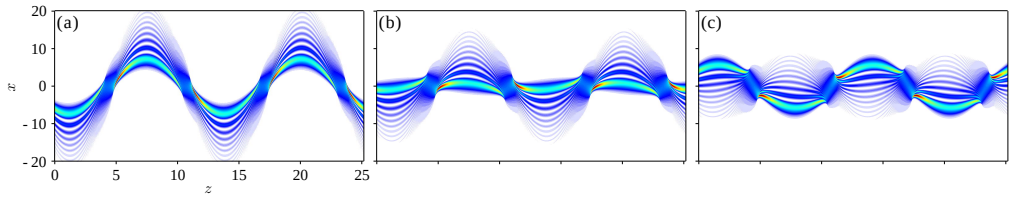

Fig. 6. Propagation of finite energy Airy beams with a quadratic chirp, for different transverse displacements. (a)-(c) $x_0 = -5$, 0, and 5, respectively (Media 5). Other parameters are $a = 0.1$, $\alpha = 0.5$, and $\beta = 0.2$.

In Fig. 6 (Media 5 is corresponding to Fig. 6(b)), we display numerical simulations of the propagating beams with quadratic chirp and different transverse displacements. One can clearly see that the phase transition points and the beam profiles at these points are in accordance with the analytical predictions.

5. Two-dimensional case

In the end, we extend the analysis to the two-dimensional (2D) case. The equation that governs the propagation of the beam can be written as

$$i\frac{\partial \psi}{\partial z} + \frac{1}{2}\left(\frac{\partial^2 \psi}{\partial x^2} + \frac{\partial^2 \psi}{\partial y^2}\right) - V(x,y)\psi = 0, \tag{20}$$

with

$$V(x) = \frac{1}{2}\alpha^2\left(x^2 + y^2\right).$$

The solution of Eq. (20) can be written as $\psi(x,y,z) = X(x,z)Y(y,z)$ and obtained using the separation of variables method [21]. Therefore, Eq. (20) can be recast into

$$i\frac{\partial X}{\partial z} + \frac{1}{2}\frac{\partial^2 X}{\partial x^2} - \frac{1}{2}\alpha^2 x^2 X - \mu X = 0, \tag{21a}$$

and

$$i\frac{\partial Y}{\partial z} + \frac{1}{2}\frac{\partial^2 Y}{\partial y^2} - \frac{1}{2}\alpha^2 y^2 Y + \mu Y = 0, \tag{21b}$$

where μ is the separation constant. If we introduce $X(x,z) = f(x,z)\exp(-i\mu z)$ and $Y(y,z) = g(y,z)\exp(i\mu z)$, Eqs. (21a) and (21b) can be rewritten as

$$i\frac{\partial f}{\partial z} + \frac{1}{2}\frac{\partial^2 f}{\partial x^2} - \frac{1}{2}\alpha^2 x^2 f = 0, \tag{22a}$$

and

$$i\frac{\partial g}{\partial z} + \frac{1}{2}\frac{\partial^2 g}{\partial y^2} - \frac{1}{2}\alpha^2 y^2 g = 0, \tag{22b}$$

#236354 - $15.00 USD Received 18 Mar 2015; revised 25 Mar 2015; accepted 26 Mar 2015; published 14 Apr 2015

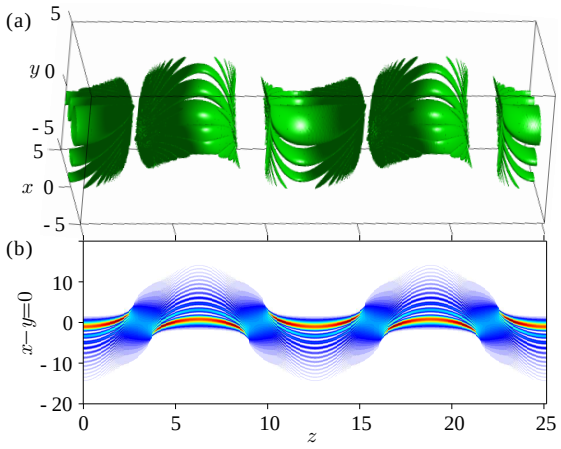

Fig. 7. Propagation of a two-dimensional finite energy Airy beam $\psi(x,y) = \exp(ax)\mathrm{Ai}(x)\exp(ay)\mathrm{Ai}(y)$ in a parabolic potential. (a) Iso-surface plot. (b) Intensity in the cross section $x-y=0$. The parameters are $a=0.1$ and $\alpha=0.5$.

which are equivalent to the two one-dimensional cases, see Eq. (1) in Sec. 2. As a result, the two-dimensional case can be reduced to the product of two independent one-dimensional cases, which makes the physical picture of the two-dimensional case quite clear.

Figure 7 depicts the propagation of the 2D Airy beam $\psi(x,y) = \exp(ax)\mathrm{Ai}(x)\exp(ay)\mathrm{Ai}(y)$ in a parabolic potential with $a=0.1$ and $\alpha=0.5$. In Fig. 7(a), one can clearly see the periodic inversion and phase transition (the gaps represent the single-peak regions) of the 2D Airy beam during propagation. We also display the intensity distribution of the beam during propagation in the cross section $x-y=0$, as shown in Fig. 7(b), which is quite similar to Fig. 1(a). Since the two-dimensional case is equivalent to a product of two one-dimensional cases, the similarity between Fig. 7(b) and Fig. 1(a) is easy to understand.

6. Conclusion

In summary, we have investigated the dynamics of finite energy Airy beams in a linear medium with an external parabolic potential, theoretically and numerically. Both one-dimensional and two-dimensional beams have been considered. We have found that the maximum intensity of the Airy beam does not exhibit harmonic oscillation, even though it moves in the parabolic potential. The whole beam exhibits phase transition at an odd integer multiple of quarters of the oscillation period, and undergoes a spatial inversion at an odd integer multiple of halves of the period. At the phase transition point, the beam becomes the Fourier transform of the initial beam, while at other places it is the Fourier transform of the initial beam with a quadratic chirp.

If the initial finite energy Airy beam carries a linear chirp, the phase transition point is not affected, but the beam at the phase transition point acquires a transverse displacement. If, on the other hand, the initial beam possesses a quadratic chirp, the phase transition point changes, but the beam profile at the point is not affected. Concerning the future outlook, it may be of interest to consider vectorial systems [30] of coupled 1D and 2D equations with a parabolic potential. Our investigation may lead to potential applications in particle manipulation, signal processing, propagation in GRIN media, and other fields.

#236354 - $15.00 USD Received 18 Mar 2015; revised 25 Mar 2015; accepted 26 Mar 2015; published 14 Apr 2015

Acknowledgment

This work was supported by the 973 Program (2012CB921804), KSTIT of Shaanxi province (2014KCT-10), NSFC (11474228, 61308015), NSFC of Shaanxi province (2014JQ8341), and the NPRP 6-021-1-005 project of the Qatar National Research Fund (a member of the Qatar Foundation).

#236354 - $15.00 USD Received 18 Mar 2015; revised 25 Mar 2015; accepted 26 Mar 2015; published 14 Apr 2015